Shear-Induced Gelation and Fracture in Micellar Solutions

Chu-heng Liu

Xerox Corporation, Wilson Center for Research & Technology, 128-33E, Webster, New York 14580

D. J. Pine

Department of Chemical Engineering, University of California, Santa Barbara, California 93106
and Department of Materials, University of California, Santa Barbara, California 93106

(Received 21 May 1996)

By direct imaging of scattered light, we observe shear-induced gelation in extremely dilute solutions of wormlike micelles. This gelation is followed by a fracture of the gel which produces extremely elastic gel bands with recoverable strains of up to 5000%. The gelation and fracture account for the unusual shear-thickening and elastic properties of these solutions.　[S0031-9007(96)01065-4]

A wide variety of surfactant molecules self-assemble in solution to form very long flexible micelles. While great progress has been made in understanding the flow behavior of such systems [1], there exists a large class of wormlike micellar solutions which exhibit anomalous behavior, namely, a dramatic increase in viscosity above a critical shear rate and a concomitant decrease in the turbulent drag. It has been suggested that these phenomena are associated with aggregation of micelles induced by the shear flow [2–4]. However, there is only indirect evidence for the existence of any shear-induced structures and very little is known about them or how they might contribute to shear thickening or drag reduction.

In this Letter, we report the first direct observation of shear-induced structures (SIS) using a novel light scattering microscopy technique. These microscopy measurements are augmented by light scattering measurements of changes in the micelle structure during shear flow, by velocity profile measurements, and by rheological data. These data show a fascinating series of shear-induced structural changes which give rise to the observed shear thickening. Moreover, our measurements indicate a correspondence between the shear-induced structural changes we measure and a number of well-documented but puzzling observations in the rheological response of the system. In particular, we have observed shear-induced gelation, fracture, and the formation of intricate cyclic patterns caused by an elastic instability.

For our studies, we used aqueous solutions of hexadecyltrimethylammoniumbromide (CTAB) and sodium salicylate (NaSal). Extreme care was taken to ensure reproducibility and allow samples to reach thermal equilibrium before each measurement. The concentrations of CTAB ranged from 30 to 2500 ppm by weight; the molar ratio of salt to surfactant was 1:1. The range of concentrations and salt-to-surfactant ratio were chosen so as to produce the strongest shear-thickening effect.

Some of the unusual flow properties of these dilute wormlike micellar solutions are illustrated in Fig. 1, where we show viscosity vs shear rate for three different concentrations of CTAB/NaSal in water. For these measurements, we used a double-wall Couette rheometer with an inner cylinder diameter of 25 mm and gap of 1 mm. For each concentration c the measured viscosity increases dramatically (up to factor of 10) as the shear rate is increased above a critical shear $\dot{\gamma}_c$ rate near 5 s^{-1}. For $\dot{\gamma} < \dot{\gamma}_c$ the viscosity is always several times greater than the viscosity of pure water (1 mPa s) and *decreases* with shear rate. This indicates that the wormlike micelles are already entangled for $c = 250$ ppm.

The inset to Fig. 1 shows a time trace of the shear stress following the sudden application of a constant shear rate $\dot{\gamma} > \dot{\gamma}_c$. After an induction period of 400–500 s, the stress begins to increase dramatically. After about 600 s, the stress ceases to grow but exhibits large slow temporal fluctuations. Fluctuations up to 50% of the steady-state stress have been reported [5,6]. Upon cessation of shear flow, the stress relaxes with a time constant of many seconds. The behaviors exhibited in Fig. 1 are typical of a wide range of wormlike micellar surfactant systems at very low concentrations. While the magnitude of these effects, e.g., the amplitude of the stress fluctuations or the duration of the induction period, vary strongly with
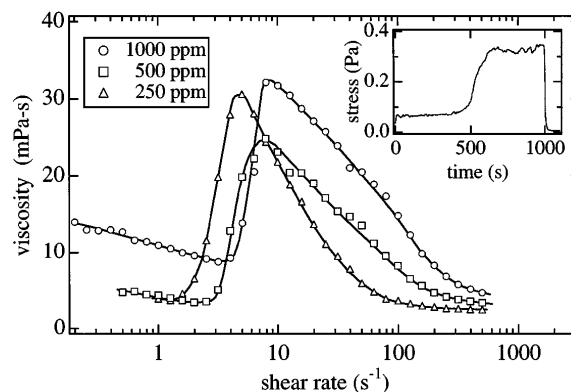
FIG. 1.　Viscosity vs shear rate for CTAB/NaSal in water. Solid lines are a guide to the eye. The inset shows the shear stress vs time following the commencement of shear flow.

concentration and shear rate, the qualitative features are common to a wide variety of systems and are consistent with previous studies [2,5,6].

To gain insight into the origin of the shear-thickening transition, we investigate flow-induced structural changes with small angle light scattering (SALS). We use a double cone geometry, illustrated in Fig. 2(a), to produce a nearly constant shear flow. Light scattered from a small region between the cones is collected for scattering angles from 1° to 10°. For such small scattering angles, the scattering vector $\mathbf{q} = \mathbf{k}_{out} - \mathbf{k}_{in}$ is nearly perpendicular to the direction of the incident light and lies almost entirely in the plane defined by the velocity and velocity gradient directions (denoted x and y, respectively). The 2D scattering pattern is recorded by a charge coupled device (CCD) camera, facilitating comparison between the time-dependent light scattering patterns of the solution and its rheological responses.

In Figs. 2(b)–2(f), we show a sequence of SALS patterns taken before and after the commencement of shear flow. Upon the commencement of shear flow, the isotropic scattering pattern of the quiescent state [Fig. 2(b)] develops symmetric lobes with intensity maxima in the second and fourth quadrants [Fig. 2(c)]. This tilted butterfly pattern, which remains unchanged for a pe-
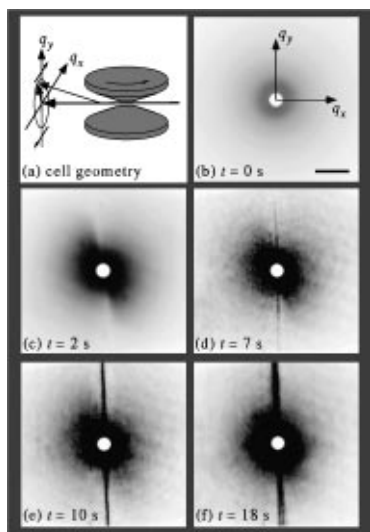
FIG. 2. (a) Double cone scattering geometry for SALS measurements. Light from a He-Ne laser passes between the two opposing cone surfaces. The scattered light is collected by an optical train and imaged onto a CCD video camera. The optical train consists of a spatial filter which ensures that only light scattered from a small region between the cones, where the shear rate is constant, is detected. (b) Equilibrium scattering pattern ($c = 1000$ ppm). The scale bar indicates $q = 1$ μm^{-1}. (c) Scattering pattern during the induction period ($\dot{\gamma} = 48$ s^{-1}). (d) Emergence of vertical streak along velocity gradient direction. (e),(f) Growth in length and intensity of streak. Note that saturation of the detector leads to an *artificial* thickening of the streak. Black denotes the highest light scattering intensity, white the lowest.

riod of time corresponding to the induction period of the stress development for this system, is characteristic of an entangled network which is weakly aligned with the principle direction of stress (45° above the x axis) for the imposed shear flow. After several seconds, a distinct short streak appears along the q_y direction. After its birth, the streak grows in length and intensity until it dominates the scattering pattern. As the streak grows, the original butterfly pattern loses its tilt and becomes nearly isotropic with only a slight elongation in the q_y direction. The appearance of this streak and the increase in scattering intensity corresponds to the beginning of the shear-thickening transition where the stress begins to grow.

The light scattering patterns reflect the spatial structure of the micelles in reciprocal space. Thus the bright streak along the q_y axis corresponds to the emergence of rodlike structures aligned along the x or flow direction in real space. The fact that the streak appears only along the q_y axis with no higher order structure at finite q_x indicates that there is no appreciable correlation in the spacing between the rodlike structures. The length of the streak along q_y is inversely proportional to the diameter of the rodlike structures, while the thickness of the streak in the q_x direction is inversely proportional to their length along the flow direction. The thickness of the streak we measure is limited by the resolution Δq of our optical train and camera. Since $\Delta q \approx 0.01$ μm^{-1}, the lower limit for the length of the rodlike structures is approximately $1/\Delta q \approx 100$ μm.

The growth in length of the streak along the q_y axis in the scattering patterns shown in Figs. 2(c) and 2(d) indicates that the rodlike structures are becoming thinner with time; their diameter changes from about 1 μm in Fig. 2(c) to less than 0.5 μm in Fig. 2(d). Measurements in our large-angle shear cell (discussed below) indicate that the scattering streak extends at least to $q_y > 5$ μm^{-1}, which means that the mean diameter of the structures ultimately thins to no more than 0.2 μm. The initial width of $\sim$1 μm of the rodlike structures indicates that the "rods" do not consist of single micelles, since these are known to be only about 5 nm in diameter [7]. The data suggest that the rodlike structures may be bundles of micelles similar to a rope consisting of entangled fibers.

The butterfly pattern which appears upon the commencement of shear flow slowly loses its tilt and becomes nearly isotropic as the streak grows in intensity. This means that more and more of the micelles are converted into the rodlike structures; a new phase of rodlike micelle structures grows out of the slightly anisotropic phase characterized by the butterfly pattern. As the streak grows in intensity, it eventually becomes unstable and begins to wobble rapidly about the q_y axis; occasionally, the streak will tumble. At the same time that the streak begins to tumble, the flow inside the cones is observed (by means of tracer particles) to become unstable, whereas previously it had been a simple lamellar shear flow. The appearance of

the unstable flow patterns is strongly correlated with the increase in the stress and the appearance of stress fluctuations in our rheological measurements.

Since the appearance and development of the flow instability is affected by the geometry of the flow cell, we chose to perform a series of structure and flow field measurements in a transparent Couette cell. The outer cylinder of the cell rotates and the inner cylinder is stationary. The cell has a diameter of 25 mm, a gap of 1 mm, and is 30 mm high, similar to the double Couette cell used for our rheological measurements [8]. Thus we expect similar behavior in the two systems.

The SALS experiments show that a new shear-induced phase coexists with the ordinary phase. To examine the spatial structure of the coexisting phases, we use a novel light scattering microscopy which results in a greater optical contrast than conventional microscopy techniques. Figure 3(a) shows the Couette shear cell and the scattering microscopy setup. We illuminate the sample with a sheet of laser light which can be oriented perpendicular to the flow direction (A) or perpendicular to the velocity gradient direction (B). The cross section of the beam has dimensions of 100 μm $\times$ 3000 μm with the larger dimension in the vorticity (z) direction of the flow field. Light scattered through an angle of 90° with respect to the incident direction is collected and imaged with a CCD video camera. In Fig. 3(b), we show a typical image of a shear-thickened sample with the imaging planes perpendicular to the flow direction. Note the existence of a bright comblike structure which extends from the stationary inner cylinder of the Couette cell. In Fig. 3(c), we show essentially the same structures but with the imaging plane parallel to the flow direction. From Fig. 3(c), we see that the bright comblike structure shown in Fig. 3(b) actually extends around the cell in the flow direction. The images show that there are regions of the sample in real space which scatter more light than other regions, indicating larger fluctuations in the micelle concentration in the bright regions than in the darker regions. Such structures do not appear in the unsheared solution but appear only when the stress begins to grow after the induction period. From observations of temporal sequences of video images we find that the comblike structure exhibits the spatial and temporal integrity of a gel.
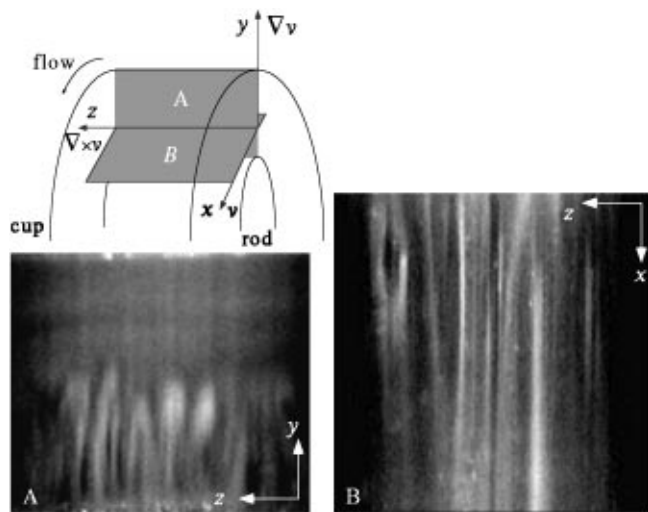
To further explore the character of the gel phase, we examine the flow field by measuring the displacement of tracer particles within the fluid using the video camera. Figure 4 shows velocity profiles taken near the middle of the glass Couette cell (orientation B in Fig. 3). The measurements are characteristic of the fully shear-thickened state in which the gel phase spans the gap of the Couette cell. The velocity fluctuations are comparable to the mean flow velocity, with alternating fast and slow moving bands. These fluctuations correspond to the comblike structure observed in Fig. 3 (albeit with fewer "tines"). The local velocity gradient along the z direction is at least 5 s^{-1} (limited by the video resolution), while the *mean* velocity gradient (along the y direction) is merely 2 s^{-1}.

Figure 4 also shows the velocity profile at the same position 2 s after the flow cell is stopped from a shear rate of 50 s^{-1}. Normally, one expects that macroscopic flow will cease and that the stress will relax diffusively when the flow cell is stopped. Here we see bands of gel material moving with different velocities and in *different directions* [9]. Even more remarkable is the fact that the recoil persists for 600 s or longer with a total recoil distance of 25 mm in the middle of the gap. This corresponds to a recoverable strain of ~5000%. This enormous elasticity of the bands supports the picture of shear-induced gelation. The fact that the sample is no

FIG. 3. (Top) Couette cell (on its side) illuminated with a sheet of light in y-z plane (A) or in x-z plane (B). (Left) Fingers of scattered light corresponding to gel structure extending from a stationary rod (bottom of image A). (Right) Streaks of scattered light corresponding to tips of gel "fingers."
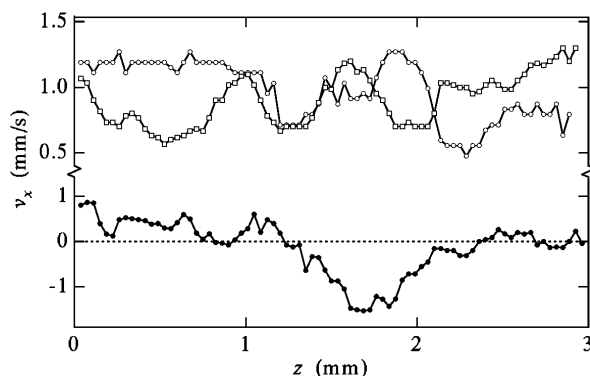
FIG. 4. (Top) Two velocity profiles of a micelle solution in high stress state taken 23 s apart in a transparent Couette cell. The velocities in the flow (x) direction are measured near the middle of the gap (see Fig. 3). (Bottom) Velocity profile shortly after the flow cell is stopped.

longer homogeneous indicates that the gel has *fractured* as it must for the arbitrarily large strains it suffers in the flow cell.

To gain further insight into the relationship between the rheological properties of the surfactant solutions and the development of the SIS, we follow the temporal development of the SIS. Since the shear-thickened state develops most slowly at low concentrations, we focus on scattering microscopy measurements at $c = 150$ ppm, where we can conveniently follow the buildup of the SIS.

Starting with a well-rested solution, we observe the accumulation of gel bands at the inner and outer boundaries after shearing for a few minutes at $\dot{\gamma} = 0.2$ s^{-1} [Fig. 5(a)]. After the shear rate is raised to 0.4 s^{-1} [Fig. 5(b)], these bands become unstable and fingerlike gel structures begin to grow from the inner stationary cylinder [Figs. 5(c) and 5(d)]. Because of the low surfactant concentration, the gel structures are more widely spaced than the tines observed at higher concentrations. The emergence of this shear-induced gel phase dramatically raises the stress in the solution and gives rise to shear thickening. As the gelation progresses, the gel fingers grow until they reach the moving outer cylinder and span the gap. At that point, they retract towards the center of the cell, apparently having been ripped apart upon spanning the gap. After retracting, they regrow towards the outer cylinder until, once again, they retract upon spanning the cell gap. *This process of growth and retraction repeats itself with a period that can be as long as several minutes and corresponds to the period of fluctuations in the stress observed in our stress measurements.* At higher surfactant concentrations, the growth and retraction process occurs more and more rapidly, as do the stress fluctuations.

It appears that shear-induced gel grows from both the inner and outer walls but that fingers develop only from the inner wall, perhaps because of an elastically driven hydrodynamic instability. It is not clear at this point, however, what role the surface plays in this process. It will be interesting to see how these observations depend on different surface treatments.

A wide variety of wormlike micellar solutions display rheological responses virtually identical to those described here. A common element in nearly all of these systems is the presence of salt anions which associate strongly with surfactant cations [7]. This seems to lead to extremely long micelles, with estimates of lengths exceeding 10 μm [7], consistent with our observations of shear thinning at the lowest shear rates for which we could make measurements (see Fig. 1).

In summary, we find that the finite induction times observed before the onset of shear thickening are associated with the buildup of long micelle bundles. This process is followed by the formation and fracture of a shear-induced gel-like structure (SIS) which grows and eventually spans the width of the cell. The growth and retraction of the SIS is consistent with the observed increase in viscosity and the fluctuations in the stress in the shear-thickened state. It also suggests that the approach to the steady-state high-stress state should depend critically on the cell geometry and, in particular, that it should take longer in cells with larger gaps, consistent with recent reports [6].
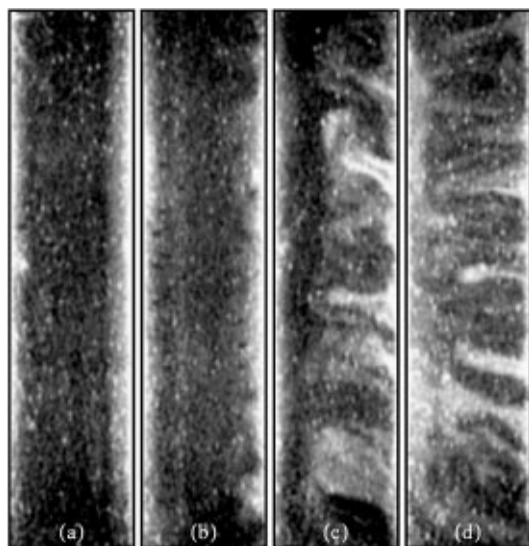
FIG. 5. Buildup of SIS structures for $c = 150$ ppm after the commencement of shear flow. The stationary rod is on the right side of each panel.

[1] M. Cates, Macromolecules **20**, 2289 (1987); M. Cates and S. Candau, J. Phys. **2**, 6869 (1990); N. Spenley, M. Cates, and T. McLeish, Phys. Rev. Lett. **71**, 939 (1993).

[2] I. Wunderlich, H. Hoffmann, and H. Rehage, Rheol. Acta **26**, 532 (1987); S. Hoffmann, A. Rauscher, and H. Hoffman, Ber. Bunsenges. Phys. Chem. **95**, 153 (1991).

[3] S. Wang, Macromolecules **25**, 7003 (1992).

[4] R. Bruinsma, W. Gelbart, and A. Benshaul, J. Chem. Phys. **96**, 7710 (1992).

[5] Y. Hu, C. Rajaram, S. Wang, and A. Jamieson, Langmuir **10**, 80 (1994); Y. Hu, S. Wang, and A. Jamieson, J. Rheol. **37**, 531 (1993).

[6] Y. Hu and E. Matthys, Rheol. Acta **34**, 450 (1995).

[7] T. Clausen *et al.*, J. Phys. Chem. **96**, 474 (1992).

[8] K. Migler, C.-h. Liu, and D. Pine, Macromolecules **29**, 1422 (1996).

[9] The intensity and texture of the light scattering images from the regions of the sample which move in opposite directions after the flow cell is stopped are indistinguishable from one another. This suggests that the regions moving in opposite directions consist of the same gel phase.